LA-UR-95-[illegible]2

Conf-9411195--2

Los Alamos National Laboratory is operated by the University of California for the United States Department of Energy under contract W-7405-ENG-36

TITLE: MEASUREMENT OF GAMMA-RAY PRODUCTION CROSS SECTIONS IN NEUTRON-INDUCED REACTIONS FOR ALUMINUM AND LEAD

AUTHOR(S): Ronald O. Nelson, Stephen A. Wender, Robert C. Haight, Phillip G. Young, Mark B. Chadwick, Andreas F. Pavlik, H. Vonach, and H. Hitzenberger

SUBMITTED TO: NEANC Specialist's Meeting on Measurement, Calculation and Evaluation of Photon Production Data
Bologna, Italy
November 9-11, 1994

Los Alamos

Los Alamos National Laboratory
Los Alamos, New Mexico 87545

FORM NO. 836 R4
ST NO 2629 5/81

Contributed paper presented at the NEANSC Specialists' Meeting on Measurement, Calculation and Evaluation of Photon Production Data, Bologna, Italy, November 9th to 11th, 1994.

MEASUREMENT OF GAMMA-RAY PRODUCTION CROSS SECTIONS IN NEUTRON-INDUCED REACTIONS FOR Al AND Pb

A. Pavlik, H. Vonach, and H. Hitzenberger
Institut für Radiumforschung und Kernphysik, Universität Wien
A-1090 Wien, Austria

and

R. O. Nelson, R. C. Haight, S. A. Wender, P. G. Young, and M. B. Chadwick*
Los Alamos National Laboratory, Los Alamos, NM 87545, U.S.A.

ABSTRACT

The prompt gamma-radiation from the interaction of fast neutrons with aluminum and lead was measured using the white neutron beam of the WNR facility at the Los Alamos National Laboratory. The samples (Al and isotopically enriched ^{207}Pb and ^{208}Pb) were positioned at about 20 m or 41 m distance from the neutron production target. The spectra of the emitted gamma-rays were measured with a high-resolution HPGe detector. The incident neutron energy was determined by the time-of-flight method and the neutron fluence was measured with a U fission chamber. From the aluminum gamma-ray spectra excitation functions for prominent gamma-transitions in various residual nuclei (in the range from O to Al) were derived for neutron energies from 3 MeV to 400 MeV. For lead (n,xnγ) reactions were studied for neutron energies up to 200 MeV by analyzing prominent gamma-transitions in the residual nuclei ^{200,202,204,206,207,208}Pb. The experimental results were compared with nuclear model calculations using the code GNASH. A good overall agreement was obtained without special parameter adjustments.

1. Introduction

Until now, almost no data existed for cross sections of neutron induced reactions for the formation of specific residual nuclei for neutron energies above 30 MeV. This is mostly due to the fact that the standard method for this purpose, the activation method, requires monoenergetic neutron sources which do not exist in this energy range. One way to study specific reaction channels at higher energies is to use a pulsed white neutron beam and to measure the prompt γ-radiation emitted in neutron-induced reactions using a high-resolution Ge-detector. The neutron energy is determined by time-of-flight (TOF) and the residual nuclei are identified by the characteristic gamma energies for transitions between low-lying levels. With the availability of the weapons neutron research (WNR) facility[1] it is possible to extend such measurements to much higher energies (several hundred MeV) than made previously at electron linear accelerators[2,3].

*Present address: Lawrence Livermore National Laboratory, Livermore, CA 94551, U.S.A.

In general, neutron-induced reactions leave the residual nucleus in a highly excited state which subsequently decays via a γ cascade to the ground state (gs) in typically 3 to 4 steps. The initial intensity distribution over a very large number of highly excited levels is collected in the first few excited levels which then decay to the ground state. Because residual nuclei are mostly formed with relatively high angular momenta, direct transitions to the 0^+ ground states of even-even nuclei are strongly inhibited. In even-even nuclei, often more than 90% of the γ cascades proceed to the ground state via the first 2^+ levels. Thus the high-resolution measurement of prompt γ production allows the identification of specific residual nuclei by the characteristic γ energies for transitions between low-lying levels, and the determination of effective cross sections for populating these levels. For even-even residual nuclei, we get approximately the total production cross section by measuring the first $2^+ \rightarrow$ gs γ-ray transition. The partial cross sections not included in this measurement result from those γ rays in the cascade that bypass the first 2^+ excited state, and those reactions that leave the residual nucleus directly in the ground state.

This technique can also be used when the residual nucleus is not even-even. In this case the partial production cross sections are obtained from the production cross sections for a given γ-ray transition, and the total production cross section must be deduced through nuclear model calculations. The partial cross section itself is of interest because it indicates the population of an individual state in the same sense as the production of isomeric states. Here, however, the states have short half-lives, whereas the less numerous isomeric states have long half-lives.

As a part of the program for white neutron source (n,xγ) measurements at the WNR facility gamma production cross sections for Al and ^{207,208}Pb were investigated. Al is monoisotopic and thus well suited for testing of model calculations and it is also of considerable interest for applications. In addition there exists a good data base for proton-induced reactions allowing detailed comparisons between the results of proton- and neutron-induced reactions.

The main purpose of the lead experiment was to test present nuclear reaction models originally developed for lower energies for neutron energies up to E_n = 200 MeV. ^{207,208}Pb samples were selected for this studies because a large amount of data already exists to restrict the parameter space for the nuclear model calculations. In addition, in the ^{208}Pb region there are very large shell effects in the nuclear level density, and it is thus possible to study the dependence of these shell effects on excitation energy with high sensitivity. Finally, there exists very good spectroscopic information on the discrete levels and γ-branching ratios for all lead isotopes reached by (n,xn) reactions up to x = 9 (^{200}Pb).

2. Experiment

The experiments were performed at the 30° left flight path of the WNR facility. The general features of the 30° left Ge spectrometer setup and of the beam pulse structure are described in Ref. 4.

Aluminum samples were irradiated at distances of 20.06 m and 41.48 m from the

neutron production target. The samples were 2 mm and 6 mm thick Al plates for the 20-m and the 41-m setup, respectively. For the lead experiment only the 41.48-m sample position was used. The enriched ^{207}Pb sample (92.78 % ^{207}Pb) had a mass of 85.64 g and consisted of three irregular shaped oval plates mounted together for a total thickness of 0.69 mm. The ^{208}Pb sample (99.56% ^{208}Pb) consisted of a flat plate with a mass of 116.3 g, 1.6 mm thick, in an oval shape approximately 9.1 cm wide and 6.6 cm high. In order to measure the contribution to the cross sections from secondary particle production and multiple reactions, the sample was subsequently rolled out to a thickness of 0.6 mm and cut into two pieces. Data were then taken with a single thin plate and also with the thin plates mounted together. The samples were mounted on a thin plastic frame and oriented at 45° with respect to the beam to reduce the attenuation of the γ-rays in the sample for detectors positioned at 90° and 125°.

Two high-purity coaxial Ge-detectors were used in each experiment. The detectors had active volumes of approximately 70 cm^3 and 140 cm^3 for the 90° and the 125° detectors, respectively. The collimators were steel tubes filled with tungsten powder, because the usual lead shielding emits the same γ rays as the isotopic lead targets when excited by scattered neutrons.

The detectors were positioned about 40.0 cm from the sample center at 90° and about 27 cm from the sample at 125°. The detector and collimator assemblies were positioned side by side to take advantage of the better shadow shielding on one side of the beam. The sample-to-detector distance was chosen to maximize the count rate while keeping the effects of pileup at a reasonable level for the 125° detector. The detector position of 125° was chosen because the value of the P_2 legendre polynomial function is zero at that angle. The usual expansion of the γ-rays angular distribution is

$$A_0(1 + a_2P_2(\cos\theta) + a_4P_4(\cos\theta) + \cdots).$$

Provided a_4 is small, the angle integrated cross section can be approximated as 4π times the measured cross section at $\theta = 125°$. Data from the 90° detector were not used in the analysis. The detector efficiencies (including the solid angle) were measured by placing calibrated ^{56}Co, ^{60}Co, ^{88}Y, ^{137}Cs, and ^{152}Eu sources at the sample center position.

The neutron flux was measured with a fission chamber. The design of the fission chamber is described in Ref. 5. The fission chamber was centered on the beam at distances of 19.30 m and 37.30 m from the production target for the 20-m and 41-m sample positions, respectively. The chamber contained a ^{238}U fission foil and for the ^{207}Pb run also a ^{235}U fission foil. A schematic diagram of the flight path collimation and shielding for the Pb sample position is shown in Fig. 1.

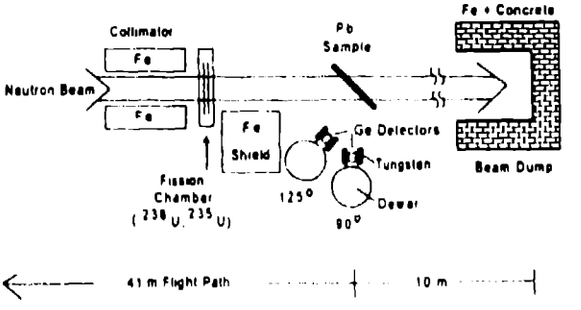

Figure 1. Experimental setup

Data were acquired using standard electronics, a CAMAC crate and a VAXstation computer. The XSYS data acquisition and analysis computer program[6] was used. Data from the Ge detectors as well as from the fission chambers were stored in event mode on disk, and sorted into 1D and 2D (neutron TOF versus pulse height) spectra. The time resolution of the 125° detector, determined from the "γ-ray flash" from the neutron production target varied from 10 ns full width at half maximum (FWHM) for E_γ = 200 keV to 5 ns FWHM for E_γ = 3 MeV. The γ-ray energy resolution obtained during the experiments was 2.8 keV FWHM at a γ-ray energy of 803 keV. The γ-ray energy resolution was limited in part by the selection of a 1 μs pulse shaping time constant which allowed high count rates without excessive pileup.

Data were taken with the samples removed for background determination. Such measurements, however, do not account for background γ rays produced by neutrons which are scattered from the sample into the collimators and detectors. To get an estimate of this background, a measurement was performed with a 0.5 mm thick tantalum plate at the sample position. The background spectra did not show any γ-ray lines overlapping in energy with the γ rays of interest.

To determine the absolute normalization of the cross sections, an experiment was performed at the Institute of Physics of the Slovak Academy of Sciences in Bratislava, Slovakia in which data were acquired at E_n = 14.7 MeV[7,8].

3. Data Reduction

3.1. General Procedure

The neutron energy range between 3 and 400 MeV for the Al measurement and between 3 and 200 MeV for the lead measurement, respectively, was divided into energy groups with increasing widths (0.25 to 50 MeV) according to the neutron energy resolution of the experiment.

The neutron fluence for each energy group was determined from the two-dimensional (neutron TOF versus fission PH) fission chamber spectra[5]. Photo-fission events induced by γ rays emitted from the neutron-production target were used as a time reference to signal the arrival of the proton beam pulse at the neutron production target. The time scale was calibrated by a time calibrator with a quartz oscillator. Alpha particles and fission fragments were distinguished by their pulse heights. A time-uncorrelated random background present in the TOF spectra was subtracted prior to sorting the fission events into neutron energy groups. The neutron fluence for each group was calculated using the cross sections for the ^{235}U(n,f) and ^{238}U(n,f) reactions given by Lisowski *et al.*[9].

Two-dimensional spectra, neutron TOF versus γ pulse-height, were recorded for the Ge detector. The "γ flash" from the neutron-production target was used as a time reference. For each neutron energy group a one-dimensional γ pulse-height spectrum was derived from the two-dimensional spectrum. Figures 2 and 3 show examples of γ spectra from the Al and the ^{208}Pb sample.

The number of counts in the γ-peak areas was obtained by adding the channel con-

tents within the peak and subtracting a smooth background. The background under a peak was obtained from polynomials fitted to suitable background regions on both sides of the peak. A linear background was used for all γ-lines with the exception of the 569.7-keV transition in ^{207}Pb, where the background could be fitted better by a quadratic polynomial.

As the choice of the peak limits and the background region is somewhat subjective, an additional uncertainty component was added quadratically to the statistical uncertainties. An estimate of this uncertainty was obtained by comparing the peak areas determined by different summing limits and background regions.

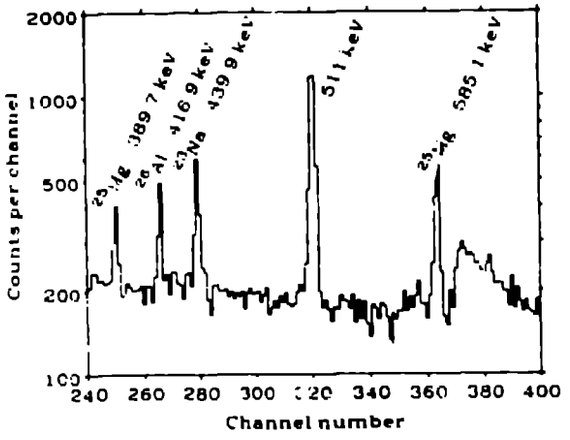

Figure 2. Part of the γ spectrum from the interaction of fast neutrons (E_n = 45 - 50 MeV) with Al

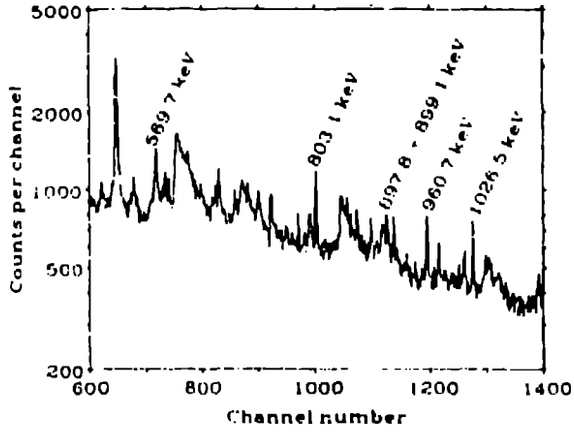

Figure 3. Part of the γ spectrum from the interaction of neutrons (E_n = 90 - 100 MeV) with ^{208}Pb.

Table I. Nuclear reactions and γ transitions in ^{27}Al(n,xγ) reactions investigated in this work.

Reaction	Residual nucleus	γ Transition investigated	Energy (keV)
^{27}Al(n,n'γ)	^{27}Al	$9/2^+ \rightarrow 7/2^+$	793.0
		$3/2^+ \rightarrow$ gs	1014.5
		$5/2^+ \rightarrow 3/2^+$	1719.5
		$7/2^+ \rightarrow$ gs	2211.
^{27}Al(n,2nγ)	^{26}Al	$3^+ \rightarrow$ gs	416.9
		$1^+ \rightarrow 0^+$	829.6
^{27}Al(n,pγ)	^{27}Mg	$5/2^+ \rightarrow 3/2^+$	955.3
		$3/2^+ \rightarrow$ gs	984.6
		$5/2^+ \rightarrow$ gs	1698.3
^{27}Al(n,pnγ) ^{27}Al(n,dγ)	^{26}Mg	$3_1^+ \rightarrow 2_1^+$	1002.5
		$2_2^+ \rightarrow 2_1^+$	1129.7
		$2_1^+ \rightarrow$ gs	1808.7
^{27}Al(n,p2nγ) ^{27}Al(n,dnγ)	^{25}Mg	$3/2^+ \rightarrow 1/2^+$	389.7
		$3/2^+ \rightarrow$ gs	974.8
^{27}Al(n,p3nγ) ^{27}Al(n,d2nγ)	^{24}Mg	$2^+ \rightarrow$ gs	1368.6
^{27}Al(n,2p3nγ) ^{27}Al(n,αnγ)	^{23}Na	$5/2^+ \rightarrow$ gs	439.9
^{27}Al(n,3p3nγ) ^{27}Al(n,αpnγ)	^{22}Ne	$2^+ \rightarrow$ gs	1274.6
^{27}Al(n,3p4nγ) ^{27}Al(n,αp2nγ)	^{21}Ne	$5/2^+ \rightarrow$ gs	350.5
^{27}Al(n,3p5nγ) ^{27}Al(n,αp3nγ)	^{20}Ne	$2^+ \rightarrow$ gs	1633.8
^{27}Al(n,4p6nγ) ^{27}Al(n,α2p4nγ) ^{27}Al(n,2α2nγ)	^{18}F	$3^+ \rightarrow$ gs	937.1
^{27}Al(n,5p5nγ) ^{27}Al(n,α3p3nγ) ^{27}Al(n,2αpnγ)	^{18}O	$2^+ \rightarrow$ gs	1982.2

Table II. Nuclear reactions and γ transitions in $^{207,208}Pb(n,xn\gamma)$ reactions investigated in this work.

Reaction	γ Transition investigated	Energy (keV)	Isomers in residual nucleus Jπ	E(keV)	$t_{1/2}$	γ Energy characteristic for isomer decay (keV)	Measured γ-production cross section
$^{207}Pb(n,2n\gamma)^{206}Pb$	$2^+ \rightarrow 0^+$ (gs)	803.1	12^+	4027.0	197 ns		
			7^-	2200.2	125 μs	516.2	σ(803.1) - σ(516.2)
$^{207}Pb(n,6n\gamma)^{202}Pb$	$2^+ \rightarrow 0^+$ (gs)	960.7	12^+	3103.4	200 ns		
			7^-	2208.5	42 ns	657.5[b]	
			9^-	2169.8	3.53 h	787.0	σ(960.7) - σ(657.5) - σ(787.0)
$^{207}Pb(n,8n\gamma)^{200}Pb$	$2^+ \rightarrow 0^+$ (gs)	1026.5	12^+	2980	194 ns		
			9^-	2176	480 ns		
			7^-	2153.7	44 ns	245.1	σ(1026.5) - σ(245.1)
$^{208}Pb(n,n'\gamma)^{208}Pb$	$3^- \rightarrow 0^+$ (gs)	2614.6		none			σ(2614.6)
$^{208}Pb(n,2n\gamma)^{207}Pb$	$\frac{5}{2}^- \rightarrow \frac{1}{2}^-$ (gs)	569.7	$\frac{13}{2}^+$	1633.4	0.805 s	1063.7	σ(569.7) - σ(1063.7)
$^{208}Pb(n,3n\gamma)^{206}Pb$	$2^+ \rightarrow 0^+$ (gs)	803.1	12^+	4027.0	197 ns		
			7^-	2200.2	125 μs	516.2	σ(803.1) - σ(516.2)
$^{208}Pb(n,5n\gamma)^{204}Pb$	$2^+ \rightarrow 0^+$ (gs)	899.1[a]	7^-	2264.2	450 ns		
			9^-	2185.7	67.2 min		
			4^+	1273.9	265 ns	374.7	σ(899.1) + σ(897.8) -σ(374.4)[a]
$^{208}Pb(n,7n\gamma)^{202}Pb$	$2^+ \rightarrow 0^+$ (gs)	960.7	12^+	3103.4	200 ns		
			7^-	2208.5	42 ns	657.5[b]	
			9^-	2169.8	3.53 h	787.0	σ(960.7) - σ(657.5) - σ(787.0)
$^{208}Pb(n,9n\gamma)^{200}Pb$	$2^+ \rightarrow 0^+$ (gs)	1026.5	12^+	2980	194 ns		
			9^-	2176	480 ns		
			7^-	2153.7	44 ns	245.1	σ(1026.5) - σ(245.1)

[a] The 899.1-keV ($2^+ \rightarrow 0^+$ in ^{204}Pb) and 897.8-keV ($3/2^- \rightarrow 1/2^-$ in ^{207}Pb) γ lines were not resolved.

[b] This line was not resolved from the 657.2-keV ($5^- \rightarrow 4^+$) transition in ^{206}Pb. A correction was made using the results of model calculations.

The γ-ray transitions analyzed in this work are listed in Tables I and II. The 569.7-keV and 897.8-keV transitions from the ^{207}Pb(n,n'γ) reaction (and the not resolved 899.1-keV transition from the ^{207}Pb(n,4nγ) reaction) were not analyzed because low energy neutrons from the preceding micropulse (frame overlap) gave significant contributions to the measured γ production cross sections. Due to the high excitation energy (2614.6 keV) of the first excited level of ^{208}Pb, the frame-overlap problem did not occur in studying the ^{208}Pb(n,n'γ) reaction.

From the peak areas, the neutron fluence, and the γ detector efficiency, relative excitation functions were derived for each γ transition analyzed. The differential cross sections at θ=125° were converted to total γ-production cross sections by multiplying them by 4π as discussed in Section 2. Correction factors for the attenuation of the γ rays within the samples were calculated using photon absorption cross sections from Ref 10.

Multiply scattered neutrons can give significant additional contributions to the measured cross sections at high incident neutron energies, especially for reactions with low thresholds. In the lead experiment this effect was estimated by comparing the γ-peak intensities obtained with samples of different thicknesses. For the aluminum measurements correction factors were estimated numerically using the results of nuclear model calculations[11] for neutron emission spectra and γ production cross sections. The correction was done for the (n,n'γ) reactions, for the ^{27}Al(n,pγ) and the ^{207,208}Pb(n,2nγ) reactions and could be neglected for all other reactions.

Because of uncertainty in our knowledge of the Ge detector dead time and the absolute flux intercepted by the irregularly shaped samples, the relative cross sections were normalized to data obtained in a separate measurement performed at the Institute of Physics of the Slovak Academy of Sciences in Bratislava with an incident neutron energy of 14.7 MeV[7,8]. Normalization factors were derived from the cross sections of prominent γ-transitions in ^{26}Mg and ^{206,207,208}Pb, respectively.

To estimate the final uncertainties of the γ production cross sections, all statistical and systematic uncertainty components were combined according to the rules of error propagation.

3.2. Corrections for Long-lived Isomers in Lead

In the residual nuclei ^{200,202,204,206,207}Pb long-lived isomeric states ($t_{1/2}$ > 2 ns) exist. When isomers are present in the cascade, a portion of the γ radiation from the first excited level → gs is not emitted promptly. Such delayed transitions cannot be properly correlated with the neutron energy because the measured TOF includes the decay delay. Therefore correction procedures had to be applied to ensure that the derived cross sections relate only to the prompt emission of γ rays. The cross sections associated with the prompt part of the γ cascade are the production cross sections for the relevant transitions minus the contributions from the long-lived isomers. According to the level schemes and γ-ray intensities[12] of ^{200,204,206,207}Pb these contributions equal γ-production cross sections related to the decay of the lowest energy isomers. Therefore the prompt γ-production cross sections for the first excited state → gs transitions can be expressed as

differences of the production cross sections for two individual transitions as listed in the last column of Table II. A similar expression can also be found for ^{202}Pb where the decay of two isomers has to be considered.

All of these measured partial cross sections (last column of Table II) are suitable quantities for direct comparison with the results of model calculations. The influence of some weaker transitions in the decay of the isomers of ^{202}Pb and ^{204}Pb was neglected because their effect is small compared to the uncertainties of this experiment and the general accuracy of nuclear model calculations. A special case is the $2_1^+ \rightarrow 0_1^+$ transition in ^{204}Pb (E_γ = 899.1 keV), which was not resolved from the E_γ = 897.8-keV $(3/2)_1^- \rightarrow$ gs transition in ^{207}Pb.

The actual correction of the measured γ-production cross sections for the delayed contributions depended on the half-lives of the various isomers. If the lifetime of the isomer is large compared to the duration of a macropulse (typically 800 μs), most of the delayed γ rays (about 98%) will be emitted between the macropulses when the detector electronics is gated off, and thus will not be counted.

For isomers with half-lives comparable to the duration of a macropulse, the delayed γ rays are observed in the measured spectra with a uniform distribution in time, and can be subtracted as a constant background. The background rate was determined from the data below the reaction threshold. This method was used to correct for the contribution of the 2200.2-keV 7$^-$ isomer ($t_{1/2}$ = 125 μs) in ^{206}Pb.

For the isomers with half-lives in the range from 40 ns to 300 ns, the delayed contributions to the measured $2_1^+ \rightarrow 0_1^+$ (gs) transitions were determined from the time distributions of the decay of the corresponding isomer. To correct for the delayed parts of the $2_1^+ \rightarrow 0_1^+$ transitions in ^{200}Pb, ^{202}Pb, and ^{204}Pb, the 245.1-keV, 657.5-keV, and 374.7-keV lines, respectively, were analyzed. These γ transitions are observed with the same delay time distributions and the same production cross sections as the parts of the $2_1^+ \rightarrow 0_1^+$ transitions that are fed via the long-lived isomers. In each time bin the intensities of these lines were subtracted from the corresponding $2_1^+ \rightarrow 0_1^+$ intensities.

Due to the only 92.78% enrichment of the ^{207}Pb sample, the measured cross sections had to be corrected for contributions from ^{208}Pb and ^{206}Pb present in the sample. These corrections were made using the measured ^{208}Pb(n,xnγ) cross sections and the results of model calculations performed with the code GNASH[13] for ^{206}Pb.

4. Results and Discussion

4.1. Aluminum Measurements

Our preliminary analysis of the data has resulted in the determination of 21 excitation functions of transitions between low-lying levels in 12 different residual nuclei for neutron energies from threshold to 400 MeV (see Table I). Three excitation functions with low, medium and high thresholds are shown in Figs. 4 - 6, together with the results of other experiments[14,15,16] (which exist in the energy range up to 14 MeV only) and the results of nuclear model calculations. The calculations were performed with the code

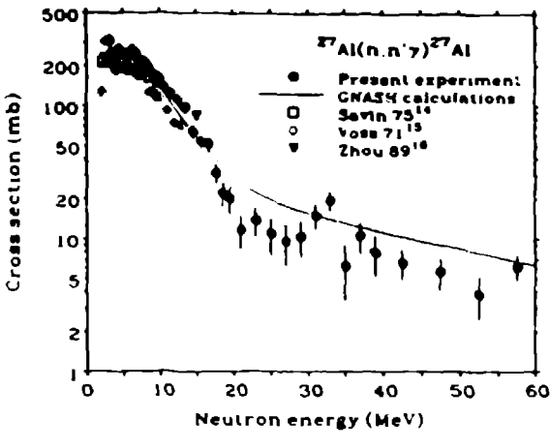

Figure 4. ^{27}Al(n,n'γ)^{27}Al cross section for the $3/2^+ \rightarrow$ gs transition (1014.5 keV).

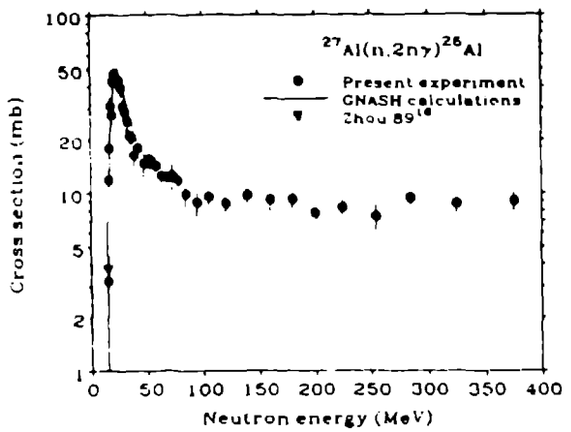

Figure 5. ^{27}Al(n,2nγ)^{26}Al cross section for the $3^+ \rightarrow$ gs transition (416.9 keV).

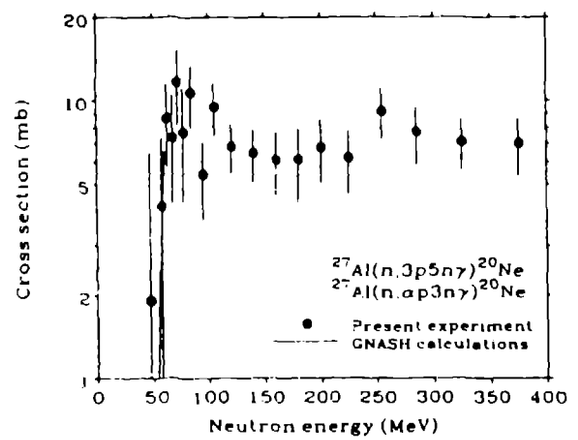

Figure 6. ^{27}Al(n,3p5nγ) and ^{27}Al(n,αp3nγ)^{20}Ne cross section for the $2^+ \rightarrow$ gs transition (1633.8 keV).

GNASH[13] for a neutron energy range up to 60 MeV. The code GNASH describes the precompound mechanism of nuclear reactions by the exciton model, the compound nucleus decay by the Hauser-Feshbach formalism, and allows the addition of contributions from direct reactions. Model parameters were not adjusted, but were kept at values typical of a large number of analyses of a variety of data at low energies in order to check the predictive power of this "standard parameter set".

As is apparent from the figures, there is good agreement between our measurements, the results reported in the literature and the calculated cross sections. This is also true for most of the excitation functions not shown in this paper, especially for all strong transitions from the first excited state to the ground state. Somewhat larger deviations (in absolute value, not in shape) up to a factor of two are observed for weaker transitions between excited levels of the investigated residual nuclei, e.g., the $3_1^+ \rightarrow 2_1^+$ transition in ^{26}Mg.

4.2. Lead Measurements

Extensive calculations of the γ-ray production cross sections studied experimentally (see Table II) were performed by means of the code GNASH. Three excitations functions are given as examples in Figs. 7-9, results of all reactions studied and a detailed discussion can be found in Ref. 17. Three extensions in the modeling of preequilibrium reactions were installed in GNASH to improve the physics for calculations at higher energies. Until now it was assumed that after the first preequilibrium particle is emit-

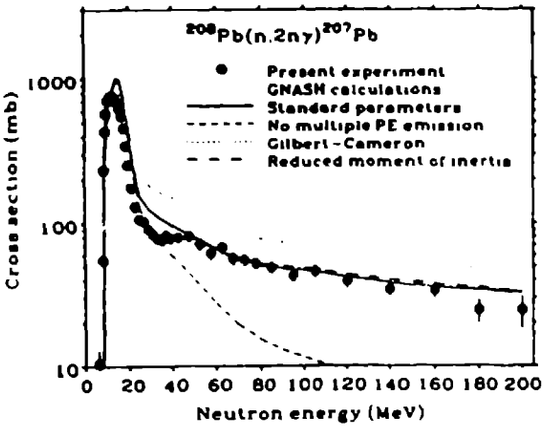

Figure 7. Prompt ^{208}Pb(n,2nγ)^{207}Pb cross section for the $(5/2)^- \rightarrow$ gs transition (569.7 keV).

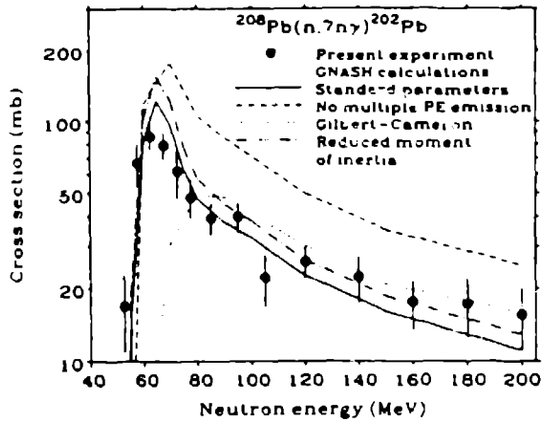

Figure 8. Prompt ^{208}Pb(n,7nγ)^{202}Pb cross section for the $2^+ \rightarrow$ gs transition (960.7 keV).

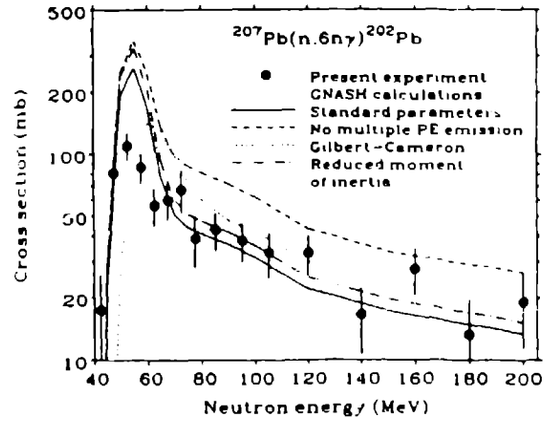

Figure 9. Prompt ^{207}Pb(n,6nγ)^{202}Pb cross section for the $2^+ \rightarrow$ gs transition (960.7 keV).

ted, the remaining particle-hole states proceed to equilibrium via a series of nucleon-nucleon collisions before decaying. We have modified this assumption to allow the particle-hole states left after primary preequilibrium emission to decay by "multiple preequilibrium" emission. The second modeling improvement was to calculate spin distributions for the residual states formed in preequilibrium reactions using angular momentum distributions based on the exciton model. And finally, we have incorporated the excitation-energy dependence of the Ignatyuk level-density formula[18] into the particle-hole state densities used in the exciton model calculations. Cross-section calculations were performed with this *a priori* "best choice" parameter set (see Ref. 17 for details). For the nuclear level densities, the Ignatyuk model was chosen instead of the simpler Gilbert-Cameron[19] and other Fermi-gas models. The energy-dependent level density parameter of the Ignatyuk model accounts for the theoretically expected disappearance of shell effects in the nuclear level densities at higher excitation energies. Within this model the nuclear moment of inertia was given the value of the full rigid body moment of inertia.

There is in general good agreement between our experiments and the calculations with the standard parameter set. There are, however , some discrepancies, ranging from about 20% to a factor of two, which need to be discussed in some detail.

There is some indication that for high-threshold reactions, (see, e.g., Fig. 8), the cross section maximum above threshold, which is predominantly due to compound nucleus decay, is less pro-

nounced than predicted theoretically. This indicates that there might be a somewhat broader distribution of excitation energies at the end of the precompound stage of the reaction than assumed in the calculations.

There is also some discrepancy between the results obtained from ^{208}Pb and ^{207}Pb concerning the cross sections for the same transitions in both ^{202}Pb and ^{200}Pb (see Figs. 8 and 9). In this case, one would expect that the calculated cross section ratios should be quite accurate because all uncertainties due to peculiarities in the decay scheme of the final nucleus should cancel. Nevertheless in both cases the ^{207}Pb cross sections in the region of the maxima of the excitation functions are considerably smaller than calculated, whereas this effect is less pronounced in ^{208}Pb. Additional measurements on ^{206}Pb could contribute to a better understanding of this effect.

In addition to the calculations performed with our "best choice" parameter set Figs. 7-9 also present a number of calculations with some modified parameter sets in order to illustrate the sensitivity of calculated cross sections to various model parameters.

The figures illustrate clearly the influence of multiple preequilibrium (PE) emission. Above neutron energies of about 40 MeV multiple precompound emission dramatically increases the (n,2nγ) and (n,3nγ) cross sections. As more high-energy neutrons are emitted, a larger fraction of the available incident energy is consumed in two or three neutron emission steps, and correspondingly the cross sections for multi-particle emission decrease. The measured data also clearly support the use of the Ignatyuk level density model for energies above 30 MeV. As seen from Fig. 8 the use of the Gilbert-Cameron level density formula results in an effective reaction threshold much higher than observed in the experiment for (n,7nγ) reactions as in the Gilbert-Cameron model considerably more energy is needed to produce a (n,xn) reaction with a specific x than in the Ignatyuk model. Calculations were also performed with a nuclear moment of inertia reduced to 60% of the rigid body value. The standard calculation gives a somewhat better overall agreement with the experimental data, but we cannot exclude the possibility of a reduced moment of inertia.

Acknowledgments

This work was supported by the Fonds zur Förderung der wissenschaftlichen Forschung in Österreich (Project P 7908-TEC), and the U.S. Department of Energy under contracts W-7405-ENG-36 and W-7405-ENG-48.

References

1. P. W. Lisowski, C. D. Bowman, G. J. Russell, and S. A. Wender, *Nucl. Sci. Eng.* **106** (1990) 208.
2. G. L. Morgan, T. A. Love, and F. G. Perey, *Nucl. Instr. Meth.* **128** (1975) 125.
3. J. K. Dickens, C. Y. Fu, D. M. Hetrick, D. C. Larson, and J. H. Todd, in *Nuclear Data for Science and Technology, (Proc. Int. Conf., Jülich, Germany, 13 - 17 May 1991)*, ed. S. M. Qaim (Springer, Berlin, 1992), p. 307.
4. R. O. Nelson, C. M. Laymon, and S. A. Wender, *Nucl. Instrum. and Meth. in Phys. Res.* **B56** (1991) 451.
5. S. A. Wender *et al.*, *Nucl. Instrum. and Meth. in Phys. Res.* **A336** (1993) 226.
6. N. R. Yoder, *XSYS, IUCF Data Acquisition Software*, (Indiana University Cyclotron Facility internal report ,1991).
7. S. Hlaváč, P. Obložinský, L. Dostal, I. Turzo, H. Vonach, A. Pavlik, and S. Simakov, submitted to *Nucl. Sci. Eng.*
8. S. Hlaváč, P. Obložinský, and S. Simakov, *Private communication*.
9. P. W. Lisowski *et al.*, in *Proc. Specialists' Meeting on Neutron Cross Section Standards for the Energy Region above 20 MeV, Uppsala, Sweden, 21 - 23 May 1991*, (Nuclear Energy Agency Nuclear Data Committee report NEANDC-305 'U', Paris, 1991), p. 177.
10. C. M. Davisson, in *Alpha-, Beta- and Gamma-ray Spectroscopy*, ed. K. Siegbahn (North Holland, Amsterdam, 1965), Vol. I, p. 827.
11. P. G. Young, *Private communication*.
12. ENSDF, *The Evaluated Nuclear Structure Data File*, Data received from National Nuclear Data Center, Brookhaven National Laboratory (1993).
13. P. G. Young, E. D. Arthur, and M. B. Chadwick, *Comprehensive Nuclear Model Calculations: Introduction to the Theory and Use of the GNASH Code* (Los Alamos National Laboratory report LA-12343-MS, Los Alamos, 1992).
14. M. V. Savin *et al.*, *Sov. J. Nucl. Phys.* **23** (1976) 269.
15. F. Voss *et al.*, in *Proc. 3rd Conference on Neutron Cross Section and Technology, Knoxville, U.S.A., 15 - 17 March 1971*, (CONF-710301, 1971), p. 218.
16. Zhou Hongyu, *Private communication* to P. Obložinský.
17. H. Vonach, A. Pavlik, M. B. Chadwick, R. C. Haight, R. O. Nelson, S. A. Wender, and P. G. Young, *Phys Rev. C* **50** (1994) 1952.
18. A. V. Ignatyuk, G. N. Smirenkin, and A. S. Tishin, *Sov. J. Nucl. Phys.* **21** (1975) 255.
19. A. Gilbert and A. G. W. Cameron, *Can. J. Phys.* **43**.(1965) 1446.